Available online at www.sciencedirect.com

jmr&t Journal of Materials Research and Technology

journal homepage: www.elsevier.com/locate/jmrt

Original Article

Characterization and determination of the gamma radiation attenuation coefficient in the W20Cu3Ni metallic alloy to be applied in the transport of radioactive substances

Armando C. Souza [a,b,*], *Flávio Aristone* [b], *Alexandre N. Santana* [b], *Adalton Miyai* [b], *Francisco C. Cione* [d], *Panos Tsakiropoulos* [c], *Jesualdo L. Rossi* [d]

[a] *UEMS, Department of Physics - CEPEMAT, CP 351, 79804-970, Units Dourados/Aquidauana, MS, Brazil*
[b] *UFMS, Institute of Physics, 79070-900, Campo Grande, MS, Brazil*
[c] *University of Sheffield, Department of Materials Science and Engineering, Sheffield S1 3JD, UK*
[d] *IPEN, Center of Technology, Science and Materials, 05508-000, Sao Paulo, SP, Brazil*

ARTICLE INFO

Article history:
Received 19 July 2022
Accepted 21 September 2022
Available online 27 September 2022

Keywords:
Attenuation coefficient
Metallic alloy
Tungsten
Radioactive transportation

ABSTRACT

The final responsibility of civil society protection regarding the nuclear sector in every country is a local/national governmental duty. The way this task is wielded changes little from country to country. The principal concern is to reduce the exposure of people to sources that eventually emit radiation. The shield used for this purpose is called biological shielding. The W20Cu3Ni metallic alloy was obtained using W powder as a matrix and the infiltrating elements Cu and Ni and subjected to sintering processes at different temperatures. All samples were analyzed by X-ray diffractometry, scanning electron microscopy (SEM). The main objective of this work is to determine the gamma radiation attenuation coefficients of the W20Cu3Ni metallic alloy subjected to different sintering temperatures. The determination of the alloy attenuation coefficient was performed using an experiment set up with a source of cobalt (Co-60), which emits characteristic energy peaks of 1.173 MeV and 1.332 MeV. The gamma rays are focused to reach the detector and the resulting photons are counted for 1800 s in three situations. Initially, the gamma rays are directed to the detector in a free path. The second experiment consists of using pure tungsten to shield the radiation, i.e., all gamma rays have to pass through it before entering the detector. Finally, the metallic alloy replaces tungsten, and the same measurements are done. Despite the amount of copper and nickel present in the final sample, the results obtained for this new metallic alloy are very satisfactory. The measurements of the gamma attenuation coefficient in the W20Cu3Ni metallic alloy at different temperatures, showed significant results, ie, a difference between 7.08% and 14.63% lower than the attenuation coefficient of pure tungsten used as a reference. Therefore, this new W20Cu3Ni metal alloy has excellent potential for application in shielding systems and in the transport of

* Corresponding author.
E-mail address: armandocirilo@yahoo.com (A.C. Souza).
https://doi.org/10.1016/j.jmrt.2022.09.083

substances with high nuclear activity used in the production of radioisotopes and radiopharmaceuticals.

1. Introduction

Regarding the nuclear sector in every country, the final responsibility for the protection of civil society is due to the local and/or national government. The way such responsibility is wielded concerning nuclear energy varies very little from one country to another. It is reasonable to outline the government directives initially before considering the technology necessary for the security of a nuclear reactor. Much of the administration and many technical requirements related to nuclear safety derive from government regulations [1].

There is a large number of functions inside the domain of radiation shielding. The principal issue is to reduce the exposure of people that have to be near the sources of radiation to the emissions. The shield used for this purpose is normally called biological shielding. The central point is to determine the necessary thickness and/or composition of the material to be used as a shield to reduce the rate and the biological dose at certain points of predetermined levels, reaching rates and maximum doses admissible for occupational exposure and the general population [1].

It can be cited here, as an example, one of the aspects influencing the shielding effect. Consider a single direction γ-*rays* beam whose intensity (or flux) is φ_0 and energy is E_0 focusing on a barrier of width a, as represented in Fig. 1. In the absence of the barrier, the exposure rate at P is given by:

$$\dot{\chi}_0 = 0,0659\varphi_0 E_0(\mu_a/\rho)^{air} mR \Big/ hr \tag{1}$$

where the unity of φ_0 is γ-*rays*/cm^2-*seg*, E_0 is in MeV, and $(\mu_a/\rho)^{air}$ is in cm^2/g, being evaluated in energy E_0. It is convenient to rewrite equation (1) as follows:

$$\dot{\chi}_0 = C\varphi_0 \tag{2}$$

in which

$$C = 0,0659\varphi_0 E_0(\mu_a/\rho)^{air} \tag{3}$$

Is a function of E_0.

When the shield is in place, the flux φ of γ-*rays* emerging out - or after - the barrier is different, i.e., smaller than the incident φ_0. The determination of the real value of $\dot{\chi}$ at the point P is solved thru numerical simulation using the XCOM software [2].

The calculation of φ would be easier if every single photon that interacts with matter disappeared completely. In this case, φ would be exactly the number of uncollected γ rays, i.e.

$$\varphi_u = \varphi_0(e)^{-\mu a} \tag{4}$$

Where μ is the total attenuation coefficient for the energy E_0. However, the incident rays do not "disappear" after each interaction. In the case of Compton effect, for example, they are merely scattered after losing some energy. In the photoelectric effect, although the incident photon is absorbed, X-rays are generally produced after the inevitable annihilation of radiation, following the production of a pair of charges. Only then the consequent spectrum of attenuation is obtained [2,3].

Recently, I. D. Tishkevich presented a work on the deposition of Bi which became of interest to the electrochemical community, due to the attenuation efficiency of the electron beam. It was determined that the optimal protetion effectiveness and mass dimensional parameters have Bi shields with a reduced thickness of 2 g/cm^2 and an attenuation coefficient of 156 [4].

Also according to I. D. Tishkevich the use of WCu composite materials with high density characteristics and reduced mass dimensions offer a very attractive alternative for lead protection due to the more ecological composite, citing as an example the W85Cu15 and W75Cu25 composites that were obtained by Solid phase synthesis showing better electronic protection [5].

Some tungsten-based alloys have excellent electronic properties. However, metals and their alloys are not without some disadvantages. One of them is its low resistance to the aggressive influence of environmental factors such as temperature, oxygen and humidity. Oxide compounds in this sense are much more stable when used up to 1000 °C. These are complex iron oxides called ferrites [6,7].

After such examples, it is justifiable that the most important part of this work is the determination of the attenuation coefficient of gamma radiation for this metallic alloy named W20Cu3Ni, which has been used as a target in an experiment prepared for the measurements of attenuation. In the setup, there is a cobalt source (Co-60) of radiation with characteristics peaks at 1.173 MeV and 1.332 MeV, coupled to a detector of gamma radiation MOD. 2M/2 BICRON (Assembled in India), counting photons during 1800 s for every series.

The matrix element of the new metallic alloy used as target is the tungsten, which presents excel properties of resistance, density, ductility, and a coefficient of attenuation in mass of approximately 0.054 cm^2/g for an energy of 1.25 MeV [8,9]. The objective of this work is focused on the characterization and determination of the gamma radiation attenuation coefficient in the new W20Cu3Ni metallic alloy, so that it can be used in the manufacture of safe packaging systems for the transport of radioactive materials, following the international safety and, particularly in Brazilian territory, under the absolute responsibility of the National Nuclear Energy Commission (CNEN).

2. Methodology and experimental setup

2.1. *Sample preparation for shielding*

A typical sample of W20Cu3Ni used as a target for shielding gamma radiation were sized 1.2 cm diameter and 0.8 cm height

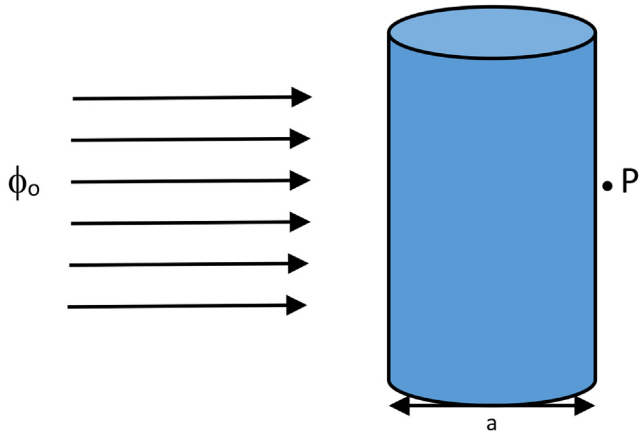

Fig. 1 – Schematic representation of one direction gamma ray beams incident on the shield barrier of width *a* [1].

after being processed using 77% of tungsten powder of appropriate distribution of particulate sizes. The grain size of the tungsten powder was in the order of 135 μm and has been mixed with 20% of Cu and 3% of Ni, all elements are 99.9% of nominal purity. The mixture has been submitted to pressing at 200 MPa. The samples used for the analysis of the attenuation coefficient were previously submitted to sintering processes and auxiliary techniques [10]. The sintering processes were carried out in a furnace limited to 1600°C, using heating ramps of 50 °C/min and performing steps from 1250 to 1400 for 1 h at each specific temperature. The furnace is coupled to a gas system where the argon flow can be modified as a function of temperature. The cooling phase for this system is not controlled, resulting in exponential decay curves [11,12]. The samples were submitted to X-ray diffraction analysis and the resulting diffractograms were analyzed with the aid of the mineral database by software, through literary consultation in the Hana Walt and Fink methods, comparison of the results with the standards produced by the Joint Committee for Powder Diffraction System (JCPDS) from the International Diffraction Data Center (ICDD). Subsequently, the samples were submitted to scanning electron microscopy (SEM) analysis for phase identification, observation of morphology, grain formation and boundaries, pore density and possible formation of intermetallic phases, in addition to analysis by energy dispersive spectrometry (EDS), qualitative and quantitative analysis of the elements present in the W20Cu3Ni samples.

2.2. *Measurements of the attenuation of gamma radiation*

The samples of such a new metallic alloy W20Cu3Ni have been submitted to measurements for determination of the attenuation coefficient of gamma radiation at the Institute of Physics of the University of Sao Paulo laboratory. It was used a system of data acquisition composed of a radioactive source of Co-60, a radiation by scintillation detector was connected to a multichannel analogic-digital converter (ADC) electronic system and to a computer with data processing software. The source of gamma radiation Co-60 presents low activity and two characteristic peaks, the first at 1.173 MeV and the second at 1.332 MeV.

The maximum value expected for the emitted radioactive energy depends on the half-life and the relation $I_I/I_0 = 1$, which indicates the absence of radioactive energy absorption by the medium. It does not depend on the radioactive sample activity. When some piece of material is positioned between the radiation detector and the Co-90 source, there are interaction of the radiation and the matter and, consequently, attenuation. This value represents the reduction of radiation by 50% of the value occurring between the peaks of photon energy emitted by the source and the photons that arrived to the detector [1,13].

For the experimental setup described above, 957 photons with 1173 keV and 701 photons with 1322 keV have been emitted, respectively, in 1800 s. Thru the results of running trials it was possible to verify that the measured coefficients of attenuation are very close to the theoretical values with excellent precision. Photons counting were always done for the 1800 s, thus contributing to increase the counting of photons emission events and, consequently, allowing to adjust the statistics of the phenomenon with better precision. Refer to the illustrative scheme for measuring the attenuation as represented in Fig. 2 [1,13].

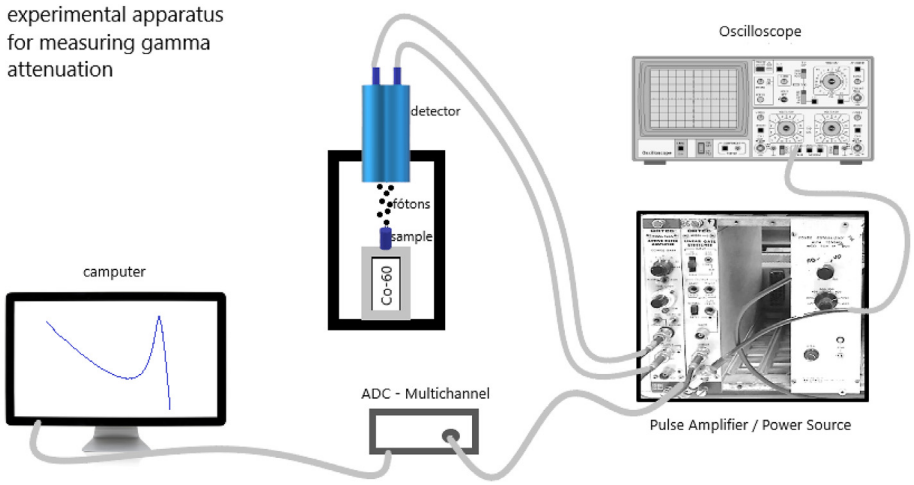

Fig. 2 – Schematic representation of the experimental setup used to measure the attenuation of gamma radiation.

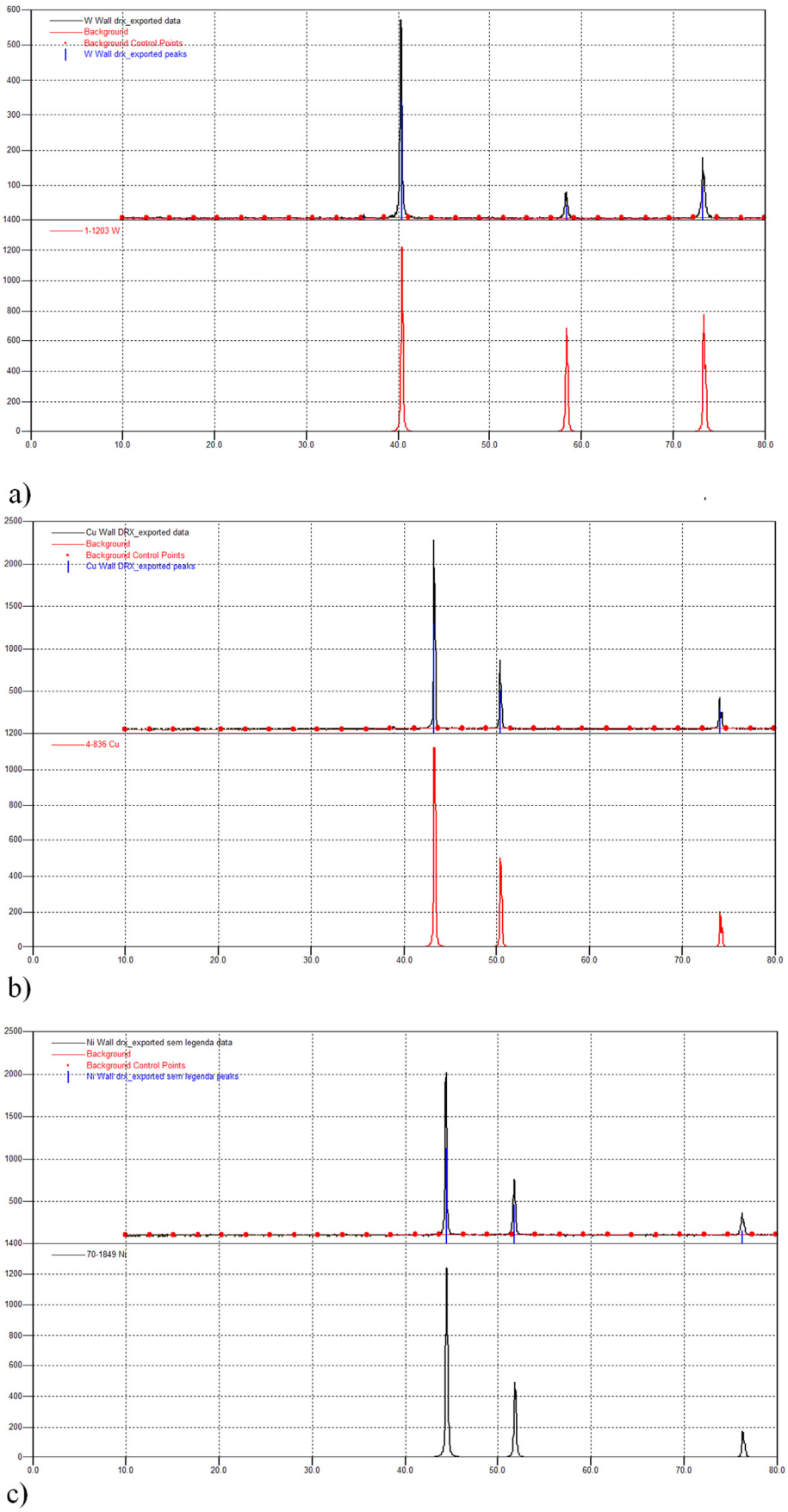

Fig. 3 – a) X-ray diffraction patterns of the elements W. b) X-ray diffraction patterns of the elements Cu. c) X-ray diffraction patterns of the elements Ni.

3. Results and discussions

3.1. Characterization of X-ray diffractometry

In Fig. 3 a), b) and c) we have the X-ray diffraction patterns of the elements W, Cu and Ni respectively, which form the metallic alloy W20Cu3Ni, where each figure contains the upper spectrum, which represents the experimental points, and the lower spectrum, which represents the comparison of the results with the standards produced by the Joint Committee for Powder Diffraction System (JCPDS) of the International Diffraction Data Center (ICDD).

Therefore, is possible to observe the variations in the peak intensities, the specific characteristics of each crystalline structure and identify the indices and the respective Miller plane references to a given reflection. From them, the interplanar distances were determined and, based on Bragg's law, the network parameters for each element, as shown in Table 1.

3.1.1. Scanning electron microscopy (SEM) analysis

The precursor chemical elements in the form of powders used to form the metal alloy were observed with the help of a scanning electron microscope (SEM). A representative micrograph of tungsten powder is shown in Fig. 4 a). Tungsten was used as the main matrix element to form the W20Cu3Ni metal alloy. This micrograph shows the morphology of the tungsten constituent particles, where we can observe the spherically symmetrical geometry and uniform sizes.

Typical micrograph for nickel powder is displayed in Fig. 4 b), which was used as an infiltrating element to form the metal alloy. In this case, the particles have irregular sponge-shaped geometries and uniform distribution throughout the sample.

The micrograph shown in Fig. 4 c) shows the result of SEM obtained for copper powder, which was later used as an infiltrating material to form the metal alloy. Copper particles have a spherical symmetry geometry of the order of 10 mm and a notable non-uniformity along the sample.

The next image, Fig. 4 d) shows a micrograph of the alloy after the grinding process using a ball mill to form a W20Cu3Ni metallic powder sample. It is possible to observe the homogeneity and uniformity of such a powder alloy that was obtained. In the sequence, this powder is initially taken to a pressing process and later submitted to a sintering process.

The samples submitted to the sintering process were analyzed, observing a sharp drop in the porosity level of the alloy as the sintering temperature increases. This effect is attributed to the more efficient thermal diffusion process during the formation of the liquid phases of Cu–Ni and W particles. The formation of the W phase, as well as the intermetallic phase Cu–Ni, in the WCuNi alloy, represent the alpha phase (α) that is associated with tungsten and the beta (β) phase associated with the binary phase of copper and nickel. Therefore, these observations showed a decrease in porosity, homogeneity and an increase in density that directly contributes to the attenuation coefficient of gamma radiation [10].

3.1.2. Attenuation coefficient of gamma radiation analysis

Two spectra used to analyze the attenuation of gamma radiation are exhibited in Fig. 5. The fulfilled black squares represent the results obtained for pure W; the empty circles are the equivalent results for the metallic alloy W20Cu3Ni sintered at 1250 °C. Both characteristic peaks, standard for the source Co-60 are clearly noticeable. The graphics show the photon intensity, i.e., the number of transmitted photons as a function of the incident energy for both shields. The metallic alloy attenuates less than the tungsten of reference, but only 14.57% and 13.68% less than the first and the second peaks, respectively. See Table 2.

Similar results are shown in Fig. 6, where the difference is the sintering temperature of the metallic alloy. In this case, the temperature was 1300 °C. The characteristic curve to evaluate the attenuation of gamma radiation was obtained as previously. The direct comparison of both results shows that the metallic alloy in this case attenuates 8.37% and 7.08% less than W for both the first and second peaks, respectively.

The spectra exhibited in Fig. 7 are used to compare the attenuation of gamma radiation by the tungsten and the new metallic alloy W20Cu3Ni sintered at 1350 °C. The two standard peaks due to the Co-60 source are present. These results indicate that the new metallic alloy attenuates 7.18% less than the first peak and 8.50% less than the second peak compared to the attenuation by the tungsten, respectively.

The last comparison is represented in Fig. 8. The spectra of gamma radiation attenuation for the tungsten and the metallic alloy W20Cu3Ni are exhibited. In this case, the sintering temperature of the alloy was 1400°C. The standard peaks of the radioactive source are present. A direct comparison shows that the alloy attenuates 14.63% less than the first

Table 1 – Crystallographic parameters.

Alloy element	2-Theta	D-Spacing (Å)	*hkl*	Intensity	Lattice parameter (Å)
W	40.339	0.2234	110	338	0.3160
CCC	58.338	0.1580	200	43	0.3160
	73.247	0.1291	211	95	0.3162
Cu	43.292	0.2088	111	1305	0.3616
CFC	50.422	0.1808	200	513	0.3616
	74.070	0.1279	220	305	0.3617
Ni	44.430	0.2037	111	1128	0.3528
CFC	51.781	0.1764	200	465	0.3528
	76.306	0.1246	220	158	0.3526

Table 2 – Obtained values for the attenuation coefficient of gamma radiation using a Co-60 as a radioactive source to hit the new metallic alloy and a standard reference tungsten used as reference.

Sample W20Cu3Ni	% of attenuation compared to standard tungsten		Attenuation coefficient of the alloy using $\mu_W = 1.044\ cm^{-1}$ as reference	
Sintering temperature °C	Peak 1.173 MeV	Peak 1.332 MeV	Peak 1.173 MeV	Peak 1.332 MeV
1250	14.57	13.32	0.891 cm^{-1}	0.901 cm^{-1}
1300	8.37	7.08	0.956 cm^{-1}	0.970 cm^{-1}
1350	7.18	8.50	0.969 cm^{-1}	0.955 cm^{-1}
1400	14.63	13.20	0.891 cm^{-1}	0.906 cm^{-1}

peak and 13.20% less than the second peak compared to the tungsten.

The metallic alloy W20Cu3Ni used as a target to analyze the radiation shielding is formed by 77% of the tungsten matrix, while the copper-nickel alloy is responsible for the resting 23%. The analyzed results corroborate the idea that different temperatures of the sintering process of W20Cu3Ni play an important role in the material's physical–chemical properties and, consequently, on the attenuation coefficients. A previous study of the microstructural evolution of the W20Cu3Ni alloy shows clear evidence of a direct accentuated reduction of the alloy porosity level whit the increasing of its sintering temperature [14]. The observed decrease in the alloy porosity is followed by an increase in the sample density and homogeneity, which would explain the different values obtained for the attenuation coefficient as a function of the temperature.

Analyzing the chemical stability of the samples, it is known that tungsten has a high chemical affinity for oxygen, especially when it interacts in an open environment and subjected to temperatures between 327°C and 400°C, forming tungsten trioxide (WO_3), but also oxidation may occur at high temperatures. To avoid any degree of oxidation of the samples and to obtain chemical stability, the sintering was carried out under a continuous flow of argon. The chemical stability occurs during the sintering process at 1250 °C, the alpha phase (α) is associated with the tungsten and the beta phase (β) represents the binary alloy Cu–Ni. The $L_{+\alpha}$ phase represents part of the Cu in the liquid phase (L) and part of the Cu solid solution in Ni [15,16]. At this temperature, the thermal diffusion of copper and nickel helps the agglutination of tungsten particles, resulting in coefficients of gamma attenuation in the order of 0.891 cm–1 and 0.901 cm-1, as exhibited in Table 2. These values have been obtained for the first and second peaks of energy of the Co-60 gamma radiation source, respectively [17,18].

A direct comparison shows that the gamma attenuation coefficients obtained for 1300 °C and 1350 °C sintering temperature are improved than those obtained for 1250 °C, as exhibited in Table 2. These results can be attributed to an enhanced process of sintering. The W20Cu3Ni metallic alloy presents smaller levels of porosity and higher mass density in

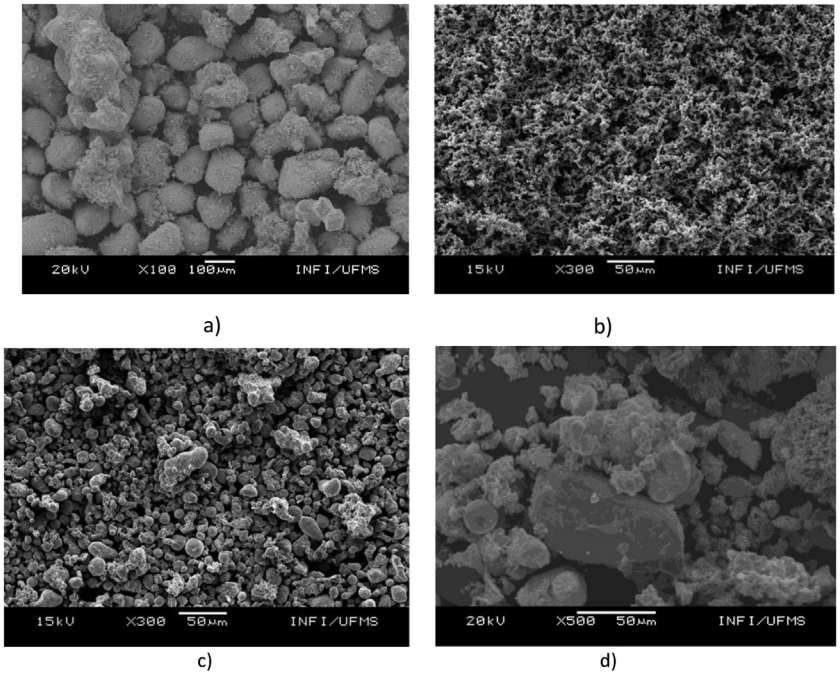

Fig. 4 – Micrograph image obtained for the a) tungsten, b) nickel, c) copper and d) metallic alloy (W20Cu3Ni) powder using SEM.

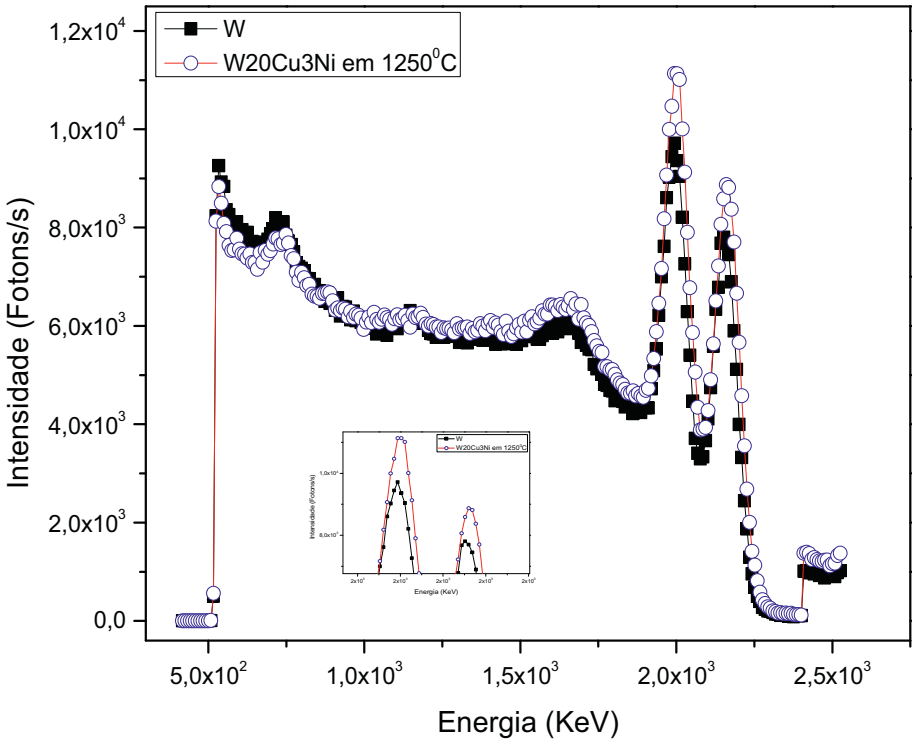

Fig. 5 – The graphics show the number of photons per second passing thru the new metallic alloy or pure tungsten as a function of the energy for comparison of the gamma radiation attenuation. The radioactive source is a stable sample of Co-60. The sintering temperature was 1250 °C. The smaller inside graphics shows the magnification of both peaks located near 2 MeV.

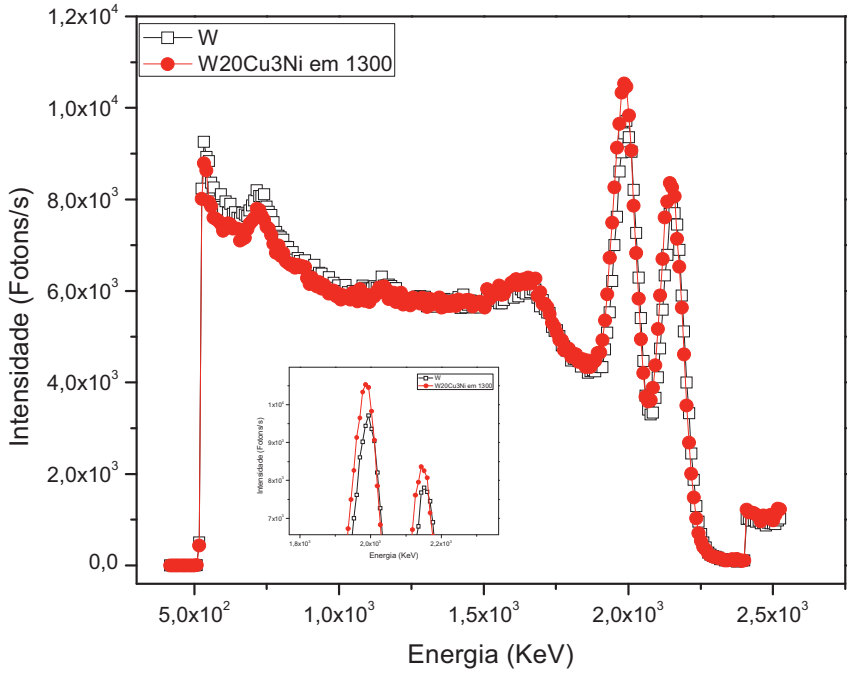

Fig. 6 – The graphics show the equivalent measurements as described previously. The sintering temperature, in this case, was set to 1300 °C. The shielding effect of the new alloy improved.

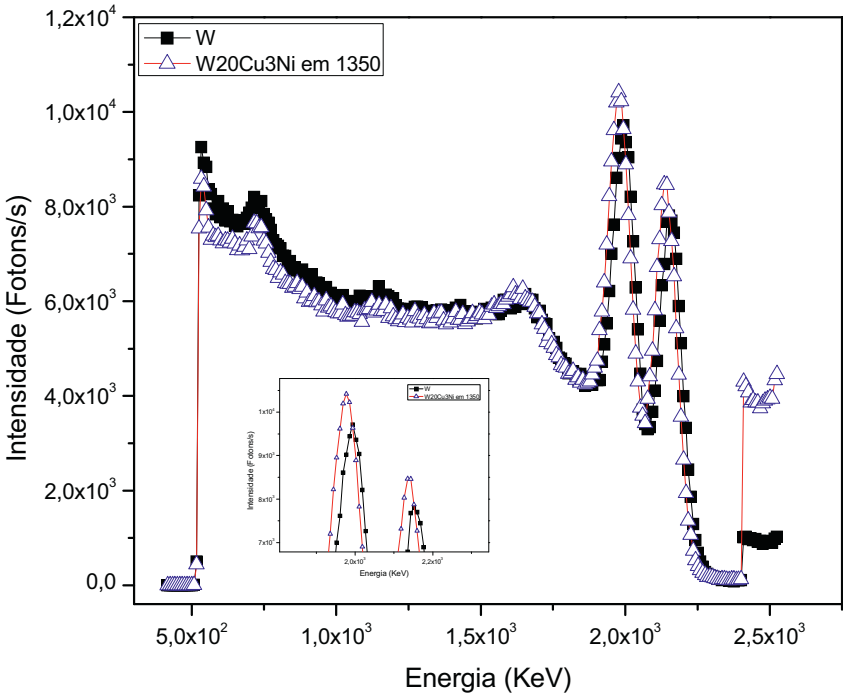

Fig. 7 – The graphics show equivalent measurements used to analyze the attenuation of gamma radiation. The sintering temperature was increased and set to 1350 °C. The shielding due to the new alloy further improved.

this range of temperature. It is a key factor in the determination of the attenuation coefficient [19,20].

The attenuation coefficients obtained for the samples sintered either at 1400 °C or 1250 °C are approximately the same, as exhibited in Table 2. This proximity in values can be explained by two complementary circumstances.

In the first case, the incomplete solubility of Cu at 1250 °C indicates that it remains a solid solution in Ni, increasing the

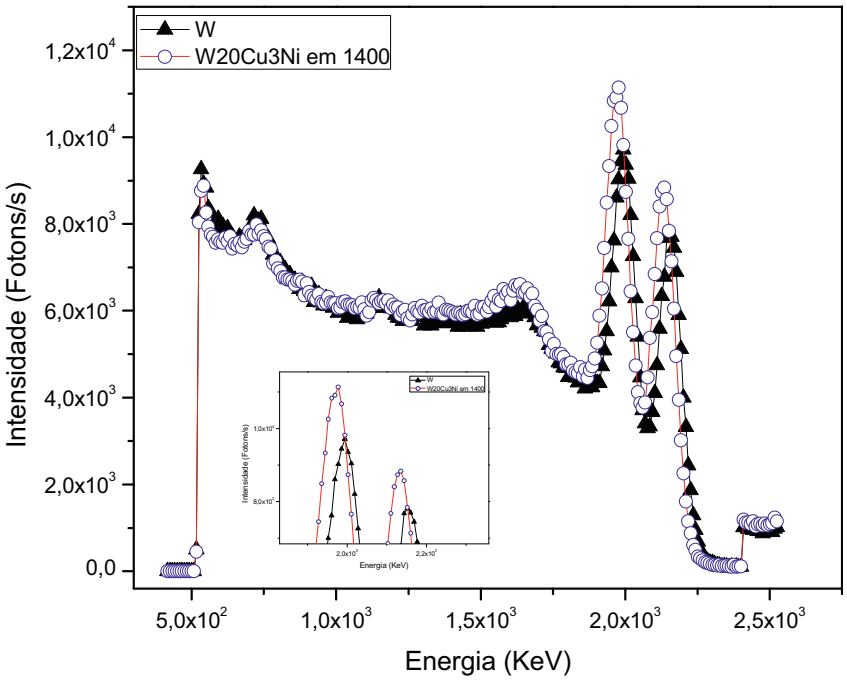

Fig. 8 – The number of photons per second as a function of the incident energy for the radiation emitted by the Co-60 source and passing thru the new metallic alloy W20Cu3Ni or thru standard pure tungsten, for comparison. The sintering temperature of the alloy was 1400 °C.

level of porosity and decreasing the mass density at this temperature. Conversely, either the Cu and the Ni have entirely entered the liquid phase at 1400 °C, therefore reducing the attenuation modulus [21].

Therefore, the results present in this paper can be considered very satisfactory regarding the metallic alloy W20Cu3Ni. Despite the considerable amount of both Cu and Ni, the attenuation coefficient of gamma radiation is only approximately 7.08% and 8.50% lower than the values obtained for the tungsten used as reference. This new alloy may become a suitable material for applications in the industry of packaging that are used for the transportation of high nuclear activity materials [18,21].

Considering the new results obtained with this new W20Cu3Ni alloy, it was possible to compare with some results in the literature, and following Jamila S. Alzahrani (2022) using an energy source of 1.173 MeV, alloys based on W, Fe, Pb and Ni presented the following attenuation coefficients, 0.8162 cm^{-1}, 0.4376 cm^{-1}, 0.5874 cm^{-1} and 0.4591 cm^{-1} respectively, showing that they are lower than the value of this new W20Cu3Ni alloy presented in this work, that is, it is more efficient in the attenuation of gamma radiation for this energy, reaching the value of 0.9690 cm^{-1} [22]. Proving to be an excellent material to be used in the manufacture of packaging for transporting a substance of high nuclear activity.

4. Conclusion

The cross section is responsible for the absorption and scattering of photons. Photons can interact with atoms in the W20Cu3Ni sample through four different processes: photoelectric, pair production, Thomson and Compton scattering. This work intends to report the determination of the gamma radiation attenuation coefficient through the cross section in a new metallic alloy W20Cu3Ni obtained from the mixture of three specific elements.: tungsten (W), copper (Cu) and nickel (Ni), submitted to different sintering temperatures, in order to compare with the attenuation capacity of standard tungsten.

The results exhibited and discussed in this paper show that the values of the attenuation coefficient of gamma radiation for the samples of the new metallic alloy W20Cu3Ni sintered at 1250 °C and 1400 °C are similar. They present a difference that is approximately 14% smaller than the values of W_{ref} for the energy of 1173 MeV, and 13% smaller for the energy of 1332 MeV. This difference is attributed, in the case of the lower temperature, to the formation of the Cu solid phase in Ni solution. The difference for higher temperature is due to the liquid phase of Cu–Ni.

The alloy presented improved coefficients of gamma radiation attenuation when the metallic alloy is sintered either at 1300 °C or 1350 °C. The results showed that it was possible to find the gamma radiation attenuation coefficients in an order of 7 and 8% lower when compared to the Wref. These results are extremely relevant, given the difficulties in producing larger tungsten-based parts and objects. Therefore, the gamma radiation attenuation coefficient in the order of 0.9690 cm−1 of the W20Cu3Ni metal alloy is superior to the W, Pb, Fe and Ni based alloys presented in the literature, which shows an excellent work and a great material. Promising for its application in the manufacture of new packages for the transport of substances of high nuclear activity used in the production of radioisotopes and radiopharmaceuticals.

Declaration of Competing Interest

The authors declare that they have no known competing financial interests or personal relationships that could have appeared to influence the work reported in this paper.

REFERENCES

[1] Lamarsh John R, Baratta Anthony J. Introduction to nuclear engineering. Third Edition. New Jersey: Prentice-Hall; 1982. p. 1–761.

[2] Berger MJ, Hubbell JH, Seltzer SM, Chang J, Coursey JS, Sukumar R, et al., XCOM: Photon Cross Sections Database. NIST Standard Reference Database 8 (XGAM), DOI:https://dx.doi.org/10.18434/T48G6X.

[3] Zivelonghi A, You JH. Mechanism of plastic damage and fracture of a particulate tungsten-reinforced copper composite: a microstructure-based finite element study. Comput Mater Sci 2014;84:318–26.

[4] Tishkevich DI, Grabchikov SS, Lastovskii SB, Trukhanov SV, Zubar TI, Vasin DS, et al. Correlation of the synthesis conditions and microstructure for Bi-based electron shields production. J Alloys Compd 2018;749:1036–42. https://doi.org/10.1016/j.jallcom.2018.03.288.

[5] Tishkevich DI, Grabchikov SS, Lastovskii SB, Trukhanov SV, Vasin DS, Zubar TI, et al. Function composites materials for shielding applications: correlation between phase separation and attenuation properties. J Alloys Compd 2019;771:238–45. https://doi.org/10.1016/j.jallcom.2018.08.209.

[6] Trukhanov AV, Turchenko VO, Bobrikov IA, Trukhanov SV, Kazakevich IS, Balagurov AM. Crystal structure and magnetic properties of the BaFe12−xAlxO19 (x=0.1–1.2) solid solutions. J Magn Magn Mater 2015;393:253–9. https://doi.org/10.1016/j.jmmm.2015.05.076.

[7] Trukhanov SV, Trukhanov AV, Kostishyn VG, Panina LV, Trukhanov AnV, Turchenko VA, et al. Investigation into the structural features and microwave absorption of doped barium hexaferrites. Dalton Trans 2017;46:9010–21. https://doi.org/10.1039/c7dt01708a.

[8] Jiqiao L, Shaoyi C, Zhiqiang Z, Haibo L, Baiyun H. Influience of tungsten oxides'characteristics on fineness, homogeneity and looseness of reduced ultrafine tungsten powder. Refractory Metals & Hard Materials 1999;17:423–9.

[9] Zakaryan M, Kirakosyan H, Aydinyan S, Kharatyan S. Combustion synthesis of W-Cu composite powders from oxide precursors with various proportions of metals. Int J Refract Metals Hard Mater 2017;64:176–83.

[10] Souza Armando C, Rossi Jesualdo L, Tsakiropoulos Panos, Aristone Flavio. Microstructural evolution of the refractory WCuNi metallic alloy. Met Mater Int 2020. https://doi.org/10.1007/s12540-020-00648-2.

[11] Chanthapan S, Kulkarni A, Singh J, Haines C, Kapoor D, et al. The sintering of tungsten powder with and without tungsten carbide additive by field assisted sintering technology. Intl Journal of Refractory Metals and Hard Materials 2012;31:114–20. https://doi.org/10.1016/j.ijrmhm.2011.09.014. ELSEVIER.

[12] Xiao Xiao W, Jiancheng T, Nan Y, Haiou Z. Novel preparation method for W-Cu composite powders. J Alloys Compd 2016;661:471–5.

[13] Nelson G, Reilly D. *"Gamma-Ray Interactions with matter,"* passive nondestructive analysis of nuclear materials. Los Alamos National Laboratory, NUREG/CR-5550; 1991. LAUR-90-732.

[14] Souza AC, Grandini CR, Florêncio O. Effect of heavy interstitials on anelastic properties of Nb-1.0 wt% Zr alloys. J Mater Sci 2008;43:1593–8.

[15] Almessiere MA, Slimani Y, Algarou NA, Vakhitov MG, Klygach DS, Baykal A, et al. Tuning the structure, magnetic and high frequency properties of Sc-doped $Sr_{0.5}Ba_{0.5}Sc_xFe_{12-x}O_{19}/NiFe_2O_4$ hard/soft nanocomposites. Adv. Electr. Mater. 2022;8:2101124. https://doi.org/10.1002/aelm.202101124.

[16] Killic M, Ozyrek D, Tuncay T. Dry sliding wear behaviour and microstructure of the W-Ni-Fe and W-Ni-Cu heavy alloys produced by powder metallurgy technique. Powder Metall Met Ceram 2016;55(1–2). May.

[17] Trukhanov SV, Troyanchuk IO, Fita IM, Szymczak H, Bärner K. Comparative study of the magnetic and electrical properties of $Pr_{1-x}Ba_xMnO_{3-\delta}$ manganites depending on the preparation conditions. J Magn Magn Mater 2001;237:276–82. https://doi.org/10.1016/S0304-8853(01)00477-2.

[18] Ibrahim H, Aziz A, Rahmat A. Enhanced liquid-phase sintering of W-Cu composites by liquid infiltration. Int J Refract Metals Hard Mater 2014;43:22–226.

[19] de Souza AC, Cione FC, Silva AC, Gouvêa AFG, Machado NGP, Raele MP, et al. Evaluation of a metal-organic composite (Tungsten-Lignin) for attenuation of gamma radiation. Math Res 2019;22. supl. 1 São Carlos 2019 Epub Sep. 02.

[20] AbuAlRoos Nadin Jamal, Azman Mira Natasha, Baharul Amin Noorfatin Ainda, Zainon Rafidah. Tungsten-based material as promising new lead-free gamma radiation shielding material in nuclear medicine. Phys Med 2020;78:48–57.

[21] Mirji R, Lobo B. Radiation shielding materials: a brief review on methods, scope and significance. In: Natl. Conf. Adv. VLS microelectron. 27th Januari 2017; 2017. P. C. Jabin Sci. Collecge, Huballi, India, no. June.

[22] Alzahrani Jamila S, Alrowaili ZA, Eke Canel, Zakaria M, Mahmoud M, Mutuwong C, et al. Nuclear shielding properties of Ni-, Fe-, Pb-, and W-based alloys. Radiat Phys Chem 2022;195:110090.